

Giant Rabi splitting in a bulk CuCl microcavity

Goro Oohata,^{1,*} Takashi Nishioka,¹ Daegwi Kim,¹ Hajime Ishihara,^{2,3} and Masaaki Nakayama¹
¹*Department of Applied Physics, Graduate School of Engineering, Osaka City University, 3-3-138 Sugimoto,
 Sumiyoshi-ku, Osaka 558-8585, Japan*

²*Department of Physics and Electronics, Graduate School of Engineering, Osaka Prefecture University,
 1-1 Gakuen-cho, Naka-ku, Sakai, Osaka 599-8531, Japan*

³*CREST, Japan Science and Technology Agency, 4-1-8 Honcho, Kawaguchi, Saitama 332-0012, Japan*
 (Received 2 June 2008; revised manuscript received 18 September 2008; published 9 December 2008)

We have investigated exciton-photon coupling phenomena in a bulk CuCl microcavity with distributed Bragg reflectors consisting of PbF₂ and PbBr₂ layers prepared by vacuum deposition. Reflectance spectra observed at various incident-light angles demonstrate the strong-coupling behavior of the exciton and photon modes; namely, the energies of reflectance dips exhibit incident-angle dependence accompanied by an anticrossing behavior peculiar to the cavity polaritons. In addition, the emission from the lower polariton branch was detected with angle-resolved photoluminescence spectroscopy. From the phenomenological analysis with a 3×3 Hamiltonian of the cavity-polariton modes originating from the Z₃ exciton, Z_{1,2} exciton, and photon, it has been revealed that the vacuum-Rabi-splitting energies are 97 and 162 meV for the Z₃ and Z_{1,2} excitons, respectively. These giant Rabi-splitting energies result from the large oscillator strengths of the relevant excitons. Furthermore, the spectral profile of reflectance is reasonably explained by calculations based on a theory of nonlocal linear optical response.

DOI: [10.1103/PhysRevB.78.233304](https://doi.org/10.1103/PhysRevB.78.233304)

PACS number(s): 78.67.-n, 71.36.+c, 71.35.-y

Exciton-photon interactions in semiconductor microcavities have attracted much attention both in physics and in device applications because of various merits of controlling optical responses.¹ In a strong-coupling regime, the mixing of an exciton and a photon results in formation of cavity polaritons, which leads to occurrence of vacuum Rabi splitting between the lower and upper polariton branches (LPB and UPB) as an anticrossing behavior. The appearance of the Rabi splitting was demonstrated in 1992 by Weisbuch *et al.*² in a GaAs quantum-well microcavity. In the second stage of the semiconductor microcavity, the parametric amplification utilizing the dispersion of the cavity polariton was discovered.^{3,4} Starting with the pioneering works, various physical phenomena were developed: parametric oscillations⁵ and polariton lasing.^{6,7} Bose-Einstein condensation of polaritons⁸⁻¹⁰ is also an interesting subject though it is still controversial.

From the viewpoint of quantum infocommunication technology, the cavity polariton can be utilized for generating entangled photon pairs.^{5,11} This proposal is based on a parametric scattering process of the cavity polaritons.^{3,12} In addition, it was theoretically predicted that the scattering process efficiently occurs via a biexciton state in a microcavity.^{13,14} The generation of entangled photon pairs was already realized in CuCl bulk crystals by utilizing biexciton-resonant hyperparametric scattering.^{15,16} We note that the binding energies of the exciton and biexciton of CuCl are 190 and 32 meV, respectively,¹⁷⁻¹⁹ which indicates that the stability of the excitonic system is very high in comparison with that in usual semiconductors. Thus, it is expected that the efficiency of the generation of entangled photon pairs will be considerably enhanced in a microcavity of CuCl. Such a CuCl microcavity, however, has not been realized until now.

In this work, we have focused on the following two subjects: the preparation of a CuCl microcavity and the optical properties of the cavity polariton. The CuCl microcavity was

prepared by vacuum deposition. We adopted a multilayer of PbF₂/PbBr₂ as a distributed Bragg reflector (DBR) because the band-gap energies of PbF₂ and PbBr₂ are higher than that of CuCl, and they are layered compounds advantageous to thin-film growth with preciseness owing to van der Waals interactions in lattice stacking.²⁰ The incident-light-angle dependence of reflectance spectra clearly exhibits a cavity-polariton dispersion. From the phenomenological analysis with a 3×3 Hamiltonian of the cavity-polariton modes originating from the Z₃ exciton, Z_{1,2} exciton, and photon, we have evaluated the following giant Rabi splitting: 97 and 162 meV for the Z₃ and Z_{1,2} excitons, respectively. Note that the Z₃ (Z_{1,2}) exciton corresponds to the split-off-hole exciton (the degenerate heavy-hole and light-hole excitons) and that the Z₃ exciton is the lowest-energy excitonic state in a CuCl crystal.^{21,22} The reflectance spectra of the CuCl microcavity are discussed with calculations based on a theory of nonlocal linear optical response.

For the sample preparation, we used a vacuum-deposition method with three sources of CuCl, PbF₂, and PbBr₂ in 7×10^{-6} Pa. The microcavity structure grown on an Al₂O₃ (0001) substrate consists of a CuCl active layer with an effective- λ length sandwiched by six periods of PbF₂/PbBr₂ as the DBR. The definition of the effective- λ length is $\lambda_{\text{eff}} \equiv \lambda_{Z(3)}/\sqrt{\epsilon_b}$, where $\lambda_{Z(3)}$ is the resonant wavelength of Z₃ exciton in vacuum and ϵ_b is the background dielectric constant. This is because the radiation field discussed here is defined by renormalizing the background dielectric constant of excitonic active layer. The designed thicknesses of the CuCl, PbF₂, and PbBr₂ layers were 164, 52, and 33 nm, respectively. The growth rates, which were monitored by a crystal oscillator during the growth process, were 0.10 nm/s for CuCl and 0.15 nm/s for PbF₂ and PbBr₂. The substrate temperature was kept at room temperature. We note that the microcavity sample was continuously grown without break-

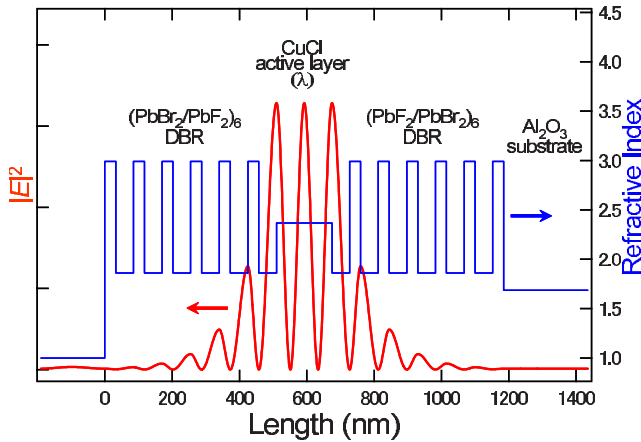


FIG. 1. (Color online) Refractive index profile of the CuCl microcavity structure together with the calculated result of the electric-field intensity ($|E|^2$) along the growth direction for normal incidence at a photon energy of 3.202 eV that is resonant with the Z_3 -exciton energy of CuCl.

ing vacuum. In order to evaluate the quality (Q) factor of the microcavity, an empty cavity, in which the active layer is replaced with a λ -length PbBr_2 , was prepared. From the transmittance spectrum of the empty cavity (not shown here), the value of the Q factor was estimated to be about 90, which is sufficient to realize the strong coupling producing the cavity polariton. In measurements of angle-resolved reflectance spectra, the probe light was a Xe lamp, and the reflectance spectrum was analyzed with a 32-cm single monochromator with a charge-coupled device as a detector, where the spectral resolution was 0.15 nm. We also measured angle-resolved photoluminescence (PL) spectra in a forward-scattering configuration, where the excitation light was introduced from the substrate side with an incidence angle of 0° . The excitation-light source was third-harmonic generation light (355 nm) of a pulsed yttrium aluminum garnet (YAG) laser, which was out of the stop band of the DBR. All the optical measurements were performed at 10 K.

Figure 1 shows the refractive index profile of the CuCl microcavity structure together with the calculated result of the electric-field intensity ($|E|^2$) along the growth direction for normal incidence at a photon energy of 3.202 eV that is resonant with the Z_3 -exciton energy of CuCl. In the calculation, we adopted a conventional transfer-matrix (TM) method, and set the active-layer thickness to the designed value of 164 nm. It is apparent that the electric field is almost confined in the DBR cavity, and the three antinodes are located on the center of the active layer and the boundary sides. Thus, we expect the occurrence of strong-coupling phenomena of cavity polaritons.

Reflectance spectra of the CuCl microcavity at various incidence angles from 0° to 60° are depicted in Fig. 2, where the dashed vertical lines indicate the energies of the Z_3 and $Z_{1,2}$ excitons: 3.202 and 3.270 eV, respectively, which are the experimental values of a simple CuCl film obtained in this work. It is apparent that seven dip structures exist in the spectra. The three dips labeled with open circles shift to the higher energy with an increase in incidence angle. These angle-dependent behaviors indicate that the three dips origi-

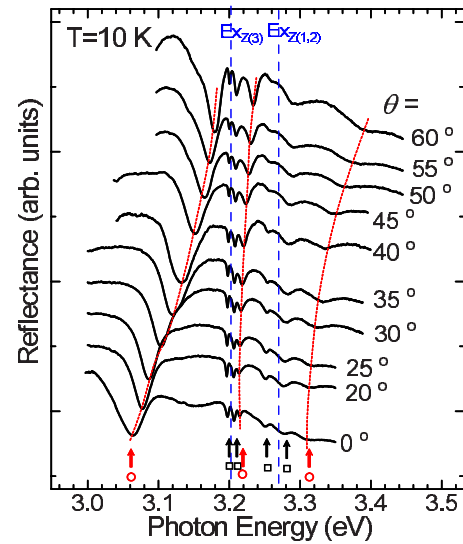


FIG. 2. (Color online) Angle-resolved reflectance spectra from the CuCl microcavity at 10 K. The dip positions labeled with open circles correspond to the strongly coupled cavity polariton, and those labeled open squares are due to weakly coupled modes. The dashed vertical lines indicate the energy positions of the Z_3 and $Z_{1,2}$ excitons of CuCl. The dotted curves are a guide for the eyes.

nate from the cavity-polariton modes. In the CuCl microcavity, the Z_3 and $Z_{1,2}$ excitons contribute to the cavity polaritons; therefore, three cavity-polariton modes should be observed. The angle-dependent three dips can be attributed to the LPB, the middle polariton branch (MPB), and the UPB in energy order. It is noted that signal reduction of UPB is due to the absorption tail of PbBr_2 which is the constituent material of DBR. In contrast, the energy shifts of other four dips are negligibly small, and they exist around the energies of the Z_3 and $Z_{1,2}$ excitons. These four dips seem to be due to weakly coupled modes. The details of the assignment described above will be discussed later with theoretical results of the spectral profile of reflectance.

Angle-resolved PL spectra of the CuCl microcavity are shown in Fig. 3. In this figure, the reflectance spectra, which were observed in the same angles, are also shown as a reference. The sharp PL band with the strongest intensity at 3.180 eV is well known as the bound-exciton band, the so-called I_1 band.¹⁹ It is reasonable that the bound-exciton PL band does not depend on the detection angle. However, the I_1 state that is a bound exciton could not be observed in reflectance spectra because the oscillator strength of the I_1 state is much smaller than that of the free exciton in CuCl. We note that a broad PL band depending on the angle is observed in the lower-energy side of the I_1 band. It is evident that the energy position of the angle-dependent PL band is identical to that of the lowest-energy dip of each reflectance spectrum. This fact indicates that the PL band originates from the LPB. In addition, two sharp PL bands were observed in the higher-energy side of the I_1 band. The energies of these two PL bands are consistent with those of the angle-insensitive two dips observed in the reflectance spectra. Therefore, the two PL bands originate from the weakly coupled modes. The sharp PL band with a weak intensity appearing at 3.142 eV is

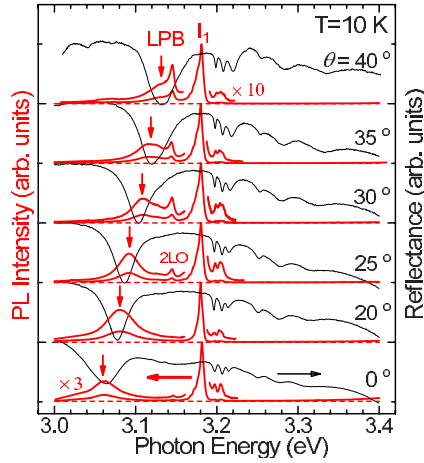


FIG. 3. (Color online) Angle-resolved PL spectra at 10 K with the corresponding reflectance spectra. The down arrows indicate the peak energy of the PL band due to the LPB. The PL band labeled I_1 is attributed to the bound exciton. The PL band labeled 2LO is the two-LO-phonon replica of the weakly coupled modes in the energy region slightly higher than the Z_3 -exciton energy.

lower in energy than the two PL bands due to the weakly coupled modes by ~ 52 meV that is twice of the longitudinal-optical (LO) phonon energy of 26 meV. This suggests that the 3.142-eV band is the two-LO-phonon replica of the weakly coupled modes.

In order to clarify the characteristics of the cavity polaritons, the energy positions of dips in the reflectance spectra are plotted as a function of incident-light angle in Fig. 4. The three dips represented as open circles clearly exhibit the angle dispersions and anticrossing behaviors. To analyze the experimental results of the incidence-angle dependence, the eigenenergies of the cavity polaritons are calculated from the phenomenological Hamiltonian considering the interaction between the cavity photon and the two exciton states of Z_3 and $Z_{1,2}$, which is given by the following equation:

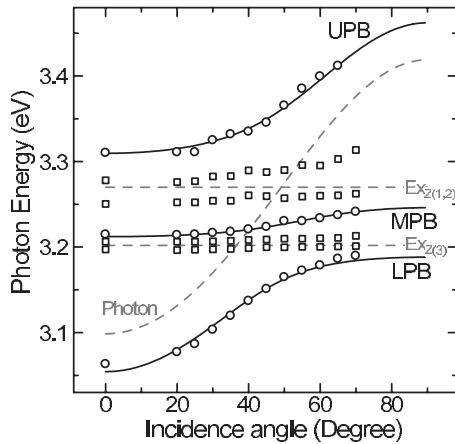


FIG. 4. Angle dependences of the energy positions of three major dips (open circles) and four minor dips (open squares) in the reflectance spectra. The solid curves are the incidence-angle dependence of the energies of the strongly coupled polariton modes calculated using the 3×3 Hamiltonian. The dashed lines represent the energies of the bare Z_3 exciton, $Z_{1,2}$ exciton, and cavity photon.

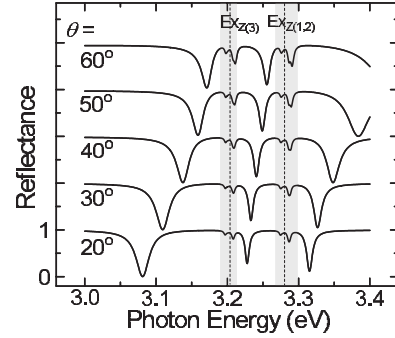


FIG. 5. Calculated reflectance spectra based on the nonlocal theory of linear optical response. The vertical dashed lines indicate the energies of the Z_3 and $Z_{1,2}$ excitons. The fine structures originating from the weakly coupled modes appear in the shaded areas in addition to the strongly coupled modes.

$$\begin{pmatrix} E_{ph} & \Omega_3/2 & \Omega_{1,2}/2 \\ \Omega_3/2 & E_{Z(3)} & 0 \\ \Omega_{1,2}/2 & 0 & E_{Z(1,2)} \end{pmatrix}, \quad (1)$$

where E_{ph} , $E_{Z(3)}$, and $E_{Z(1,2)}$ are the energies of the cavity photon, Z_3 , and $Z_{1,2}$ excitons, respectively. The symbol of Ω_3 ($\Omega_{1,2}$) is the vacuum Rabi-splitting energy between the photon and Z_3 ($Z_{1,2}$) exciton. The energy of the cavity photon is written as $E_{ph}(\theta) = E_0(1 - \sin^2 \theta / n_{eff}^2)^{-1/2}$, where θ is the external reflectance angle, E_0 represents the resonance energy of the cavity at $\theta = 0^\circ$, and n_{eff} is the effective refractive index of the cavity. Since the weakly coupled modes are out of the strong-coupling regime, we do not consider them in the analysis with the phenomenological Hamiltonian for the strong-coupling cavity modes. The solid curves in Fig. 4 indicate the calculated results of the cavity-polariton eigenvalues. It is obvious that the energies of the angle-dependent three dips are well explained by the calculated results; namely, those are attributed to the strongly coupled cavity polaritons. In this calculation, Ω_3 , $\Omega_{1,2}$, and E_0 are fitting parameters: $\Omega_3 = 97$ meV, $\Omega_{1,2} = 162$ meV, and $E_0 = 3.099$ eV. As a result, we demonstrate that the giant Rabi splitting is realized in the CuCl microcavity. In addition, the effective thickness of the CuCl layer is estimated to be 169 nm from the value of E_0 , which is slightly different from the designed value of 164 nm.

Here, we compare the present results of the vacuum-Rabi-splitting energies with reported values in bulk GaN microcavities: 30–50 meV.^{23,24} It is noted that the binding energy and oscillator strength of the exciton in GaN are the largest in semiconductors used as active layers of microcavities. The Rabi-splitting energy of an exciton, Ω , usually depends on the oscillator strength.²⁵ The excitonic oscillator strength can be estimated from the splitting energy between the longitudinal and transverse excitons on the basis of a dielectric-function model.²⁶ According to the parameter values for GaN,²⁷ the oscillator strength of the A exciton is 3.3×10^4 meV². In CuCl, the oscillator strength of Z_3 exciton is 2.1×10^5 meV².¹⁹ Thus, the larger oscillator strength leads to the giant Rabi-splitting energy in the CuCl microcavity.

Finally, we discuss the reflectance spectra of the CuCl microcavity from the calculation based on a theory of non-local linear optical response, the so-called nonlocal theory.²⁸ For the precise discussion of the polariton mode in the bulk cavity, we have to consider the spatial structures of the photon field and the excitonic wave function because a long-wavelength approximation is unsuitable for the bulk active layer.^{28,29} Figure 5 shows calculated reflectance spectra based on the nonlocal theory including a center-of-mass quantization effect on excitons peculiar to the bulk cavity. In this calculation, the damping constant of the excitonic response and the Q factor of the modeled DBR were phenomenologically set to 2 meV and ~ 90 , respectively. It is evident from Fig. 5 that the seven dip structures observed in the reflectance spectra (Fig. 2) are reproduced in the calculated spectra. Namely, the angle-dependent three reflectance dips are conclusively attributed to the strongly coupled modes: LPB, MPB, and UPB. In addition, the four minor dips around the energies of the Z_3 and $Z_{1,2}$ excitons clearly appear in the spectra. It is considered that these structures are the

weakly coupled modes. The weakly coupled modes originate from the spatial mismatch between the cavity field and the wave function of the center-of-mass quantized exciton mode.^{29,30}

In summary, we have prepared the effective- λ CuCl microcavity including the PbF₂/PbBr₂ DBR, and realized the giant Rabi splitting of the cavity-polariton modes consisting of the Z_3 exciton, $Z_{1,2}$ exciton, and photon. The angle dependence of the reflectance-dip energies of the strongly coupled modes are well explained by the phenomenological 3×3 Hamiltonian: the resultant Rabi-splitting energies are 97 meV for the Z_3 exciton and 162 meV for the $Z_{1,2}$ exciton, the so-called giant Rabi splitting. The spectral profiles of reflectance including weakly coupled modes are reasonably explained by the theory of nonlocal linear optical response.

This research was supported by a Grant-in-Aid for Creative Scientific Research (Grant No. 17GS1204) from the Japan Society for the Promotion of Science.

-
- *Present address: Department of Physical Science, Graduate School of Science, Osaka Prefecture University, 1-1 Gakuen-cho, Nakaku, Sakai, Osaka 599-8531, Japan. oohata@p.s.osakafu-u.ac.jp
- ¹*The Physics of Semiconductor Microcavities*, edited by B. Deveaud (Wiley, Weinheim, 2007).
 - ²C. Weisbuch, M. Nishioka, A. Ishikawa, and Y. Arakawa, *Phys. Rev. Lett.* **69**, 3314 (1992).
 - ³P. G. Savvidis, J. J. Baumberg, R. M. Stevenson, M. S. Skolnick, D. M. Whittaker, and J. S. Roberts, *Phys. Rev. Lett.* **84**, 1547 (2000).
 - ⁴M. Saba *et al.*, *Nature (London)* **414**, 731 (2001).
 - ⁵C. Diederichs, J. Tignon, G. Dasbach, C. Ciuti, A. Lemaitre, J. Bloch, P. Roussignol, and C. Delalande, *Nature (London)* **440**, 904 (2006).
 - ⁶H. Deng, G. Weihs, D. Snoke, J. Bloch, and Y. Yamamoto, *Proc. Natl. Acad. Sci. U.S.A.* **100**, 15318 (2003).
 - ⁷S. Christopoulos *et al.*, *Phys. Rev. Lett.* **98**, 126405 (2007).
 - ⁸H. Deng, G. Weihs, C. Santori, J. Bloch, and Y. Yamamoto, *Science* **298**, 199 (2002).
 - ⁹J. Kasprzak *et al.*, *Nature (London)* **443**, 409 (2006).
 - ¹⁰R. Balili, V. Hartwell, D. Snoke, L. Pfeiffer, and K. West, *Science* **316**, 1007 (2007).
 - ¹¹C. Ciuti, *Phys. Rev. B* **69**, 245304 (2004).
 - ¹²D. Strelakov and J. Dowling, *J. Mod. Opt.* **49**, 519 (2002).
 - ¹³H. Ajiki and H. Ishihara, *J. Phys. Soc. Jpn.* **76**, 053401 (2007).
 - ¹⁴H. Oka and H. Ishihara, *Phys. Rev. Lett.* **100**, 170505 (2008).
 - ¹⁵K. Edamatsu, G. Oohata, R. Shimizu, and T. Itoh, *Nature (London)* **431**, 167 (2004).
 - ¹⁶G. Oohata, R. Shimizu, and K. Edamatsu, *Phys. Rev. Lett.* **98**, 140503 (2007).
 - ¹⁷T. Mita, K. Sôtome, and M. Ueta, *Solid State Commun.* **33**,

- 1135 (1980).
- ¹⁸B. Hönerlage, A. Bivas, and Vu Duy Phach, *Phys. Rev. Lett.* **41**, 49 (1978).
- ¹⁹M. Ueta, H. Kanzaki, K. Kobayashi, Y. Toyozawa, and E. Hanamura, *Excitonic Process in Solids* (Springer, New York, 1986).
- ²⁰M. Nakayama, D. Kim, and H. Ishihara, *Phys. Rev. B* **74**, 073306 (2006).
- ²¹A. Goldmann, *Phys. Status Solidi B* **81**, 9 (1977).
- ²²H. Overhof, *Phys. Status Solidi B* **97**, 267 (1980).
- ²³N. Antoine-Vincent, F. Natali, D. Byrne, A. Vasson, P. Disseix, J. Leymarie, M. Leroux, F. Semond, and J. Massies, *Phys. Rev. B* **68**, 153313 (2003).
- ²⁴I. R. Sellers, F. Semond, M. Leroux, J. Massies, P. Disseix, A. L. Henneghien, J. Leymarie, and A. Vasson, *Phys. Rev. B* **73**, 033304 (2006).
- ²⁵M. S. Skolnick, T. A. Fisher, and D. M. Whittaker, *Semicond. Sci. Technol.* **13**, 645 (1998).
- ²⁶C. F. Klingshirn, *Semiconductor Optics* (Springer, New York, 2007), Chap. 4, p. 81.
- ²⁷R. Stępniewski, K. P. Korona, A. Wyszemolek, J. M. Baranowski, K. Pakula, M. Potemski, G. Martinez, I. Grzegory, and S. Porowski, *Phys. Rev. B* **56**, 15151 (1997).
- ²⁸K. Cho, *Optical Response of Nanostructures: Microscopic Non-local Theory* (Springer, New York, 2003).
- ²⁹H. Ishihara and J. Kishimoto, *Proceedings of the 25th International Conference on the Physics of Semiconductors*, Osaka, 2000, edited by N. Miura and T. Ando (Springer, Berlin, 2001), p. 685.
- ³⁰Y. Chen, A. Tredicucci, and F. Bassani, *Phys. Rev. B* **52**, 1800 (1995).